A&A 409, L9–L12 (2003)
DOI: 10.1051/0004-6361:20031238

Astronomy & Astrophysics

Letter to the Editor

Gamma-ray bursts and X-ray melting of material to form chondrules and planets

P. Duggan[1], B. McBreen[1], A. J. Carr[2], E. Winston[1], G. Vaughan[3], L. Hanlon[1], S. McBreen[1], L. Metcalfe[4], Å. Kvick[3], and A. E. Terry[3]

[1] Department of Experimental Physics, University College Dublin, Dublin 4, Ireland
[2] Mechanical Engineering Department, University College Dublin, Dublin 4, Ireland
[3] European Synchrotron Radiation Facility, BP 220, 38043 Grenoble Cedex, France
[4] XMM-Newton science Operations Center, European Space Agency, Villafranca del Castillo, 28080 Madrid, Spain

Received 19 June 2003 / Accepted 8 August 2003

Abstract. Chondrules are millimeter sized objects of spherical to irregular shape that constitute the major component of chondritic meteorites that originate in the region between Mars and Jupiter and which fall to Earth. They appear to have solidified rapidly from molten or partially molten drops. The heat source that melted the chondrules remains uncertain. The intense radiation from a gamma-ray burst (GRB) is capable of melting material at distances up to 300 light years. These conditions were created in the laboratory for the first time when millimeter sized pellets were placed in a vacuum chamber in the white synchrotron beam at the European Synchrotron Radiation Facility (ESRF). The pellets were rapidly heated in the X-ray and gamma-ray furnace to above 1400 °C melted and cooled. This process heats from the inside unlike normal furnaces. The melted spherical samples were examined with a range of techniques and found to have microstructural properties similar to the chondrules that come from meteorites. This experiment demonstrates that GRBs can melt precursor material to form chondrules that may subsequently influence the formation of planets. This work extends the field of laboratory astrophysics to include high power synchrotron sources.

Key words. methods: laboratory – gamma rays: bursts – X-rays: general planetary systems: formation – solar system: general

1. Introduction

The production of chondrules is an important stage in processes leading to the formation of planets (Cuzzi et al. 2001). Many proposals (Boss 1996) have been made for the transient heat source that melted the precursor material to form chondrules including nebular lightning (Desch & Cuzzi 2000) and activities associated with the young Sun (Shu et al. 2001; Feigelson et al. 2002). Almost all proposed heat sources (Rubin 2000; Boss 1996; Jones et al. 2000) are local to the solar nebula, one exception being the proposal (McBreen & Hanlon 1999; Duggan et al. 2001) that the chondrules were flash heated to melting point by a nearby GRB when the iron all through the precursor material efficiently absorbed X-rays and low energy γ-rays. The distance to the source could be up to 300 light years ($\sim$100 pc) for a GRB with an isotropic output of 10^{46} J (Piran 1999; Mészáros 2002). This distance limit was obtained using the minimum value of 2×10^6 J kg^{-1} required to heat and melt the precursor grains (Wasson 1993) and is equivalent to an enormous energy deposition of 10^8 J m^{-2}. The complex time profiles of short and long GRBs are well described by lognormal distributions (McBreen et al. 2001; Quilligan et al. 2002).

The timing, duration and conditions that led to the formation of chondrules in the solar nebula are poorly understood. The properties and thermal histories of the chondrules have been inferred from an extensive series of experiments (Connolly et al. 1998; Lofgren & Lanier 1990; Connolly et al. 1994; Cohen et al. 2000). Their mineralogy is dominated by olivine ((Mg, Fe)$_2$SiO$_4$) and pyroxene ((Mg, Fe)SiO$_3$) both being solid solutions with a wide range in composition. This diversity is consistent with the melting of heterogeneous solids or dust balls. Crystal structures and morphologies are used to limit the temperature range and rate of cooling during chondrule formation. Backscattered electron microscope images of two typical chondrules that we obtained from the Allende meteorite with barred and porphyritic textures are shown in Fig. 1.

2. Experimental method

It is now possible to create the astrophysical conditions near a GRB source in the laboratory due to the development of powerful synchrotrons. The ESRF has a 6 GeV, third-generation synchrotron capable of generating the required power. A wiggler device was inserted and used to create X-rays in the range 3–200 keV. The 24-pole wiggler has a characteristic energy of 29 keV at a minimum wiggler gap of 20.3 mm. Time was

Send offprint requests to: B. McBreen,
e-mail: brian.mcbreen@ucd.ie

Table 1. Elemental oxide compositions of three types of precursor material in weight percentages and the calculated liquidus temperatures. The compositions are the same as listed (Yu & Hewins 1998) except that the small amounts of K_2O (<0.11%) were not included and magnetite (Fe_3O_4) was used in place of FeO.

	Type IA	Type IAB	Type II
SiO_2	45.4	47.2	49.2
TiO_2	0.1	0.1	0.1
Al_2O_3	4.9	9.7	4.1
Fe_3O_4	8.3	6.6	21.3
MnO	0.1	0.1	0.1
MgO	37.4	30.7	22.7
CaO	2.5	3.5	0.2
Na_2O	1.3	2.1	2.3
Liquidus temperature	1692 °C	1577 °C	1509 °C

awarded on the ID 11 white beam to test the prediction that large fluxes of X-rays and γ-rays could melt millimetre sized dust grains and hence extend the use of high power synchrotron sources to laboratory astrophysics (Remington et al. 1999).

The composition of chondrules varies widely and a classification system based on the iron content is often used (McSween 1977; Yu & Hewins 1998). Type IAB chondrules have low iron content while type IA and type II have increasing amounts of iron. The pellets were made from a mixture of elemental oxides with weight percentages as given in Table 1 for the three precursors types. The major effect of including more iron is to reduce the magnesium content and the liquidus temperature of the material. The oxides, without the volatile Na_2O, were mixed and heated to 400 °C in an alumina crucible for 13 hours. The powders after heating had a mass loss of about 5%, due to moisture loss and reduction of the elemental oxides. After cooling, Na_2O was added to the mixture. The powder was pressed into cylindrical pellets of diameter 3 mm and height of 3 mm.

Each pellet was placed in a graphite crucible inside an evacuated container and inserted into the path of the white X-ray beam. The size of the beam was 2 mm × 1.5 mm. The synchrotron beam entered the vacuum chamber through a Kapton window of thickness 0.05 mm. The pressure in the container was between 10^{-2}–10^{-3} mbar, which is typical of planetary forming systems. In a few cases the residual air in the vacuum chamber was replaced with hydrogen. During the heating cycle the temperature of the pellet was measured using a Raytex MR1SCSF pyrometer with a range from 1000 °C to 3000 °C. The pyrometer was located outside the lead shielding and viewed the sample via a mirror through a glass window on the top of the vacuum container and at right angles to the X-ray beam. This window had to be replaced on several occasions during the experiment because of darkening caused by radiation damage. The sample was also monitored with a camera that viewed it through the pyrometer optics. The pellets were rapidly heated in the X-ray and γ-ray furnace to temperatures above 1400 °C (Fig. 2). During the heating and melting process the pellets bubbled, moved about and sometimes ejected small drops of iron rich material. The melted samples were kept at the maximum temperature for a duration of 10 s to 300 s and cooled when the power in the beam was reduced by widening the magnets of the wiggler. The beam was removed when the temperature dropped below 1000 °C. The samples cooled rapidly to yield 2–3 mm diameter black spherules.

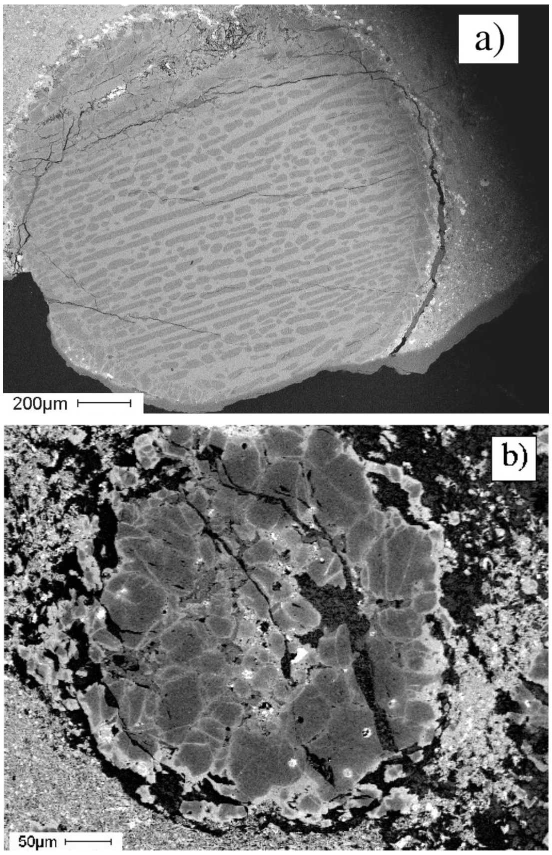

Fig. 1. Backscattered electron microscope images of two chondrules from the Allende meteorite. Phases with higher atomic number are brighter in color. The dark grey grains are elongated olivine crystals in **a)** and porphyritic crystals in **b)** where the brighter regions are the interstitial glassy material. The diameters of the chondrules are about 1 mm and 0.6 mm and are surrounded by matrix material in the meteorite.

A Huber model 642 Guinier X-ray powder diffractometer with monochromatic Cu Kα_1 radiation was used for powder diffraction. Aluminium foil was placed between the sample and detector to reduce the fluorescent background from iron. The crystal phases were identified using the JCPDS Powder Diffraction File. Crystal structures were refined using Rietveld analysis in the range $20^\circ < 2\theta < 100^\circ$ using Rietica (Hunter 1998; Hill & Howard 1987). For angular calibration and quantitative phase analysis a known mass of high-purity silicon (9% to 16% by mass depending on the sample) was added as an internal standard to the powdered sample. Refined structural variables included lattice parameters, atomic coordinates, metal site occupancies and isotropic temperature factor; non-structural variables included scale factors, background correction and peak shape. Absorption effects were treated as though they were part of the overall isotropic temperature factor (Scott 1981).

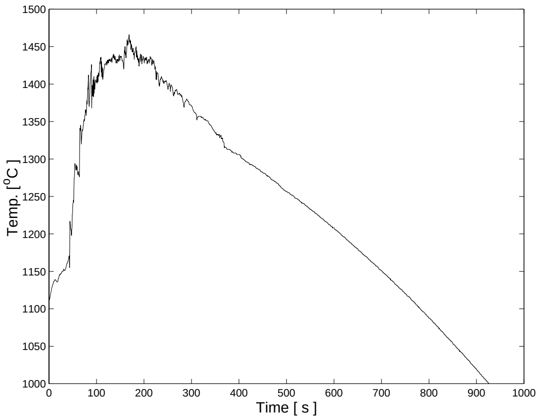

Fig. 2. The temperature profile of a typical sample in the synchrotron experiment. The reason for the high initial temperature is that 1000 °C is the minimum value read by the pyrometer. The temperature rose rapidly to above 1000 °C when the beam shutter was opened.

3. Results

A total of 24 samples were melted and cooled in the radiation beam. Backscattered electron microscope images of three samples are given in Fig. 3. One sample (Fig. 3a) has olivine crystals orientated in a random pattern whereas the sample in Fig. 3b has a barred olivine texture. The sample in Fig. 3c has porphyritic microstructure.

There was a general tendency for the microstructure of the samples to reflect the liquidus temperature (Yu & Hewins 1998). Type IA samples have the highest liquidus temperature of 1692 °C (Table 1). The type IA samples were predominantly porphyritic in texture with smaller crystals while IAB were about equal mixture of porphyritic and acicular olivine whereas acicular olivine predominated in type II. The type IA samples with highest liquidus temperature had more nuclei throughout the partial melt at the start of cooling on which the crystals could grow (Rubin 2000). The greater number of nucleation sites resulted in more crystals with smaller dimensions. Type II samples had the least number of nucleation sites resulting in fewer but larger crystals. The faster the cooling rate the more imperfect the crystals that formed. There is not a perfect match between the microstructure of chondrules (Fig. 1) and the samples produced in the synchrotron beam (Fig. 3). The final texture of samples depends on a range of factors (Rubin 2000; Connolly et al. 1998; Lofgren & Lanier 1990) such as the precursor composition, maximum temperature, rate of cooling and duration of heating at maximum temperature. Further experiments are needed to explore a wider range in parameter space to obtain more observational constraints on the process.

The Rietveld plot of one type II sample is given in Fig. 4. The R values, relating the observations to the model, for type IA samples were typically $R_p = 6.5\%$ for the profile and $R_{wp} = 8.2\%$ for the weighted profile and for type II samples were $R_p = 2.2\%$ and $R_{wp} = 2.8\%$ indicating very acceptable fits. The sample in Fig. 3a had olivine with weight percentage of 56.6% with the remainder being amorphous while the type II sample shown in Fig. 4 had olivine (86.2 wt-%), magnetite (7.2 wt-%) with the remainder being amorphous. The Bragg R_B factors for the individual crystalline phases were also very acceptable with values less than 4%. Refining the site occupancy factors for the two magnesium and iron sites allowed the calculation of stoichiometry of the olivine as $Mg_{1.92}Fe_{0.08}SiO_4$, (i.e. almost pure forsterite) for the type IA sample (Fig. 3a) and $Mg_{1.72}Fe_{0.28}SiO_4$ for the type II sample (Fig. 4). The higher iron content of the type II olivine reflects the greater amount of iron in the starting mixture.

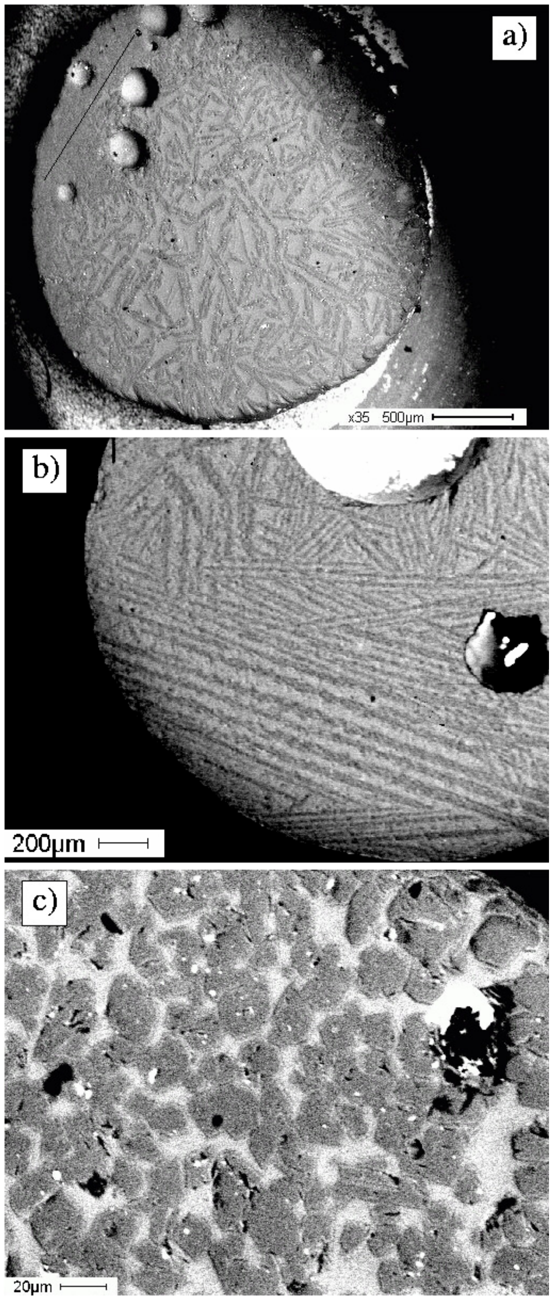

Fig. 3. Backscattered electron microscope images of three melted samples from the synchrotron experiment. **a)** Cross section of a complete sample with randomly orientated olivine crystals and type IA precursor composition. **b)** Section of a sample with barred olivine crystals and type II precursor composition. **c)** Section of a sample with porphyritic crystals and type IAB precursor composition. The samples in **a)** and **c)** have cavities of size <500 mm. Cavities have been observed (Maharaj & Hewins 1994) in other experimentally produced samples and are caused by trapped gases and incomplete melting.

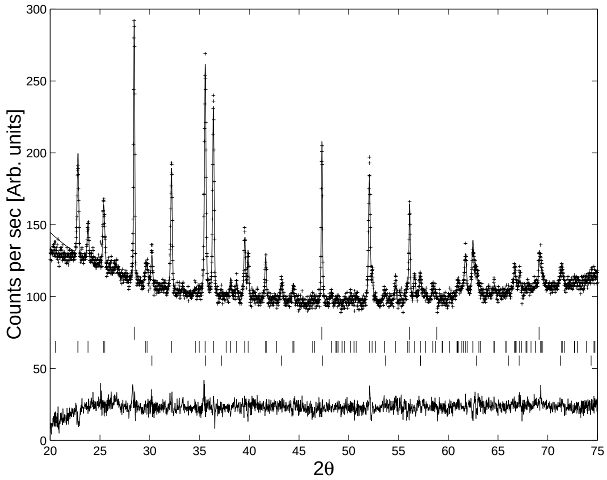

Fig. 4. X-ray diffraction pattern of a type II sample. The data are plotted with crosses and the calculated profile is shown as a continuous line. The three sets of vertical bars in the middle of the figure are the calculated reflection positions for silicon (top), olivine (middle) and magnetite (bottom). The residuals between the data and the calculated profile are shown at the bottom of the figure indicating a very good match.

4. Discussion

This experiment demonstrates that GRBs can melt precursor dust balls to form chondrules in nearby planetary forming systems. Once formed, the chondrules can move through the gas more freely and coagulate to form the building blocks of planets (Cuzzi et al. 2001). GRBs with durations greater than 2 s are associated with supernovae in massive stars and the formation of Kerr black holes (Popham et al. 1999; McBreen et al. 2002). The discovery of more than 100 extra-solar giant planets has opened a range of questions regarding the mechanisms of planetary formation (Santos et al. 2003; Laughlin 2000). The probability that any planetary forming system will be blasted by a nearby GRB has been estimated (McBreen & Hanlon 1999; Scalo & Wheeler 2002) to be about 0.1%. In the solar neighbourhood, 7% of stars with high metallicity harbour a planet whereas less than 1% of stars with solar metallicity seem to have a planet (Santos et al. 2003). The GRB method seems to be only one of the mechanisms involved because of the high percentage of stars with planets. There is a further difficulty for the model in the case of our solar system because most chondrules were melted more than once requiring a repeating process (Rubin 2000; Wasson & Rubin 2003). However the formation of planetary systems may be enhanced by the presence of a nearby GRB which will form chondrules across the whole nebula at essentially the same time (McBreen & Hanlon 1999) but would require a range of assumptions about the location of the dust in the disk to account for the properties of chondrules in different classes of chondrites. Advances in the methods of detecting remnant GRBs and planetary systems may reveal a link between them in our galaxy.

A GRB can reveal planetary forming systems in other galaxies because there will be short duration (~1 hour) bursts of infrared radiation from the melted dust when chondrules form across the whole nebula. These infrared bursts can occur for up to several hundred years after the GRB when the expanding shell of radiation melts the dust in planetary forming systems. However the GRB should be in a nearby galaxy to detect the faint infrared bursts with powerful telescopes such as the overwhelmingly large telescope and the Next Generation Space Telescope.

Acknowledgements. The University College Dublin group thank Enterprise Ireland for support. We thank Alan Rubin for his insightful comments.

References

Boss, A. P. 1996, in Chondrules and the Protoplanetary Disk., ed. R. H. Hewins, R. H. Jones, & E. R. D. Scott (Cambridge: Cambridge University Press), 257

Cohen, B. A., Hewins, R. H., & Yu, Y. 2000, Nature, 406, 600

Connolly, H. C., Jones, B. D., & Hewins, R. H. 1998, Geochim. Cosmochim. Acta, 62, 2725

Connolly, H. C. J., Hewins, R. H., Ash, R. D., et al. 1994, Nature, 371, 136

Cuzzi, J. N., Hogan, R. C., Paque, J. M., & Dobrovolskis, A. R. 2001, ApJ, 546, 496

Desch, S. J., & Cuzzi, J. N. 2000, Icarus, 143, 87

Duggan, P., McBreen, B., Hanlon, L., et al. 2001, in Gamma-ray Bursts in the Afterglow Era, ed. E. Costa, J. Hjorth, & F. Frontera (Springer Verlag), 294

Feigelson, E. D., Garmire, G. P., & Pravdo, S. H. 2002, A&A, 572, 335

Hill, R. J., & Howard, C. J. 1987, J. Appl. Crystallogr., 20, 467

Hunter, B. 1998, International Union of Crystallography Commission on Powder Diffraction Newsletter, 22, 21

Jones, R. H., Lee, T., Connolly, H. C., Love, S. G., & Shang, H. 2000, Protostars and Planets IV, 927

Laughlin, G. 2000, ApJ, 545, 1064

Lofgren, G., & Lanier, A. B. 1990, Geochim. Cosmochim. Acta, 54, 3537

Mészáros, P. 2002, ARA&A, 40, 137

Maharaj, S. V., & Hewins, R. H. 1994, Geochim. Cosmochim. Acta, 58, 1335

McBreen, B., & Hanlon, L. 1999, A&A, 351, 759

McBreen, S., McBreen, B., Hanlon, L., & Quilligan, F. 2002, A&A, 393, L15

McBreen, S., Quilligan, F., McBreen, B., Hanlon, L., & Watson, D. 2001, A&A, 380, L31

McSween, H. Y. 1977, Geochim. Cosmochim. Acta, 41, 477

Piran, T. 1999, Phys. Rep., 314, 575

Popham, R., Woosley, S. E., & Fryer, C. 1999, ApJ, 518, 356

Quilligan, F., McBreen, B., Hanlon, L., et al. 2002, A&A, 385, 377

Remington, B. A., Arnett, D., Drake, R. P., & Takabe, H. 1999, Science, 284, 1488

Rubin, A. E. 2000, Earth-Science Rev., 50, 3

Santos, N. C., Israelian, G., Mayor, M., Rebolo, R., & Udry, S. 2003, A&A, 398, 363

Scalo, J., & Wheeler, J. C. 2002, ApJ, 566, 723

Scott, H. G. 1981, Acta. Cryst., A37, 456

Shu, F. H., Shang, H., Gounelle, M., Glassgold, A. E., & Lee, T. 2001, ApJ, 548, 1029

Wasson, J. T. 1993, Meteoritics, 28, 14

Wasson, J. T., & Rubin, A. E. 2003, Geochim. Cosmochim. Acta, 67, 2239

Yu, Y., & Hewins, R. H. 1998, Geochim. Cosmochim. Acta, 62, 159